

Two kinds of high-contrast optical filters for the detection of Stokes and anti-Stokes photons from cesium ensemble

Tingting LIU, Qiangbing LIANG, Jun HE, and Junmin WANG*

State Key Laboratory of Quantum Optics and Quantum Optics Devices (Shanxi University),
and Institute of Opto-Electronics, Shanxi University
No.92 Wu Cheng Road, Taiyuan 030006, Shanxi Province, P. R. China

ABSTRACT

We report experimental investigations of two kinds of high-contrast optical filters by utilizing a laser-pumped atomic vapor and properly-designed Fabry-Perot bulk etalon, which are based on the demand of the detection of quantum correlated Stokes and anti-Stokes photon pairs in a Λ -type three-level atomic ensemble, respectively. Laser-pumped cesium (Cs) atomic filter achieves typical peak transmission $\sim 74.3\%$ and the distinction ratio between excitation channel and 9.19GHz- frequency-detuned signal channel is ~ 26.7 dB at 47.15 °C. The transmission peak can be tuned within the range of Doppler line-width of Cs D₂ line. The temperature-stabilized narrow-band etalon filter with dozens of GHz resonant transmission tunability is realized with typical peak transmission of $\sim 91.7\%$ and the distinction ratio between pump and signal channel of ~ 27.5 dB. These techniques are useful for atom-photon interaction experiments, especially for Stokes and anti-Stokes photon pairs generation experiments based on collective Raman excitation of Cs atomic ensemble.

Keywords: atomic filter, etalon filter, Stokes photons, anti-Stokes photons, collective excitation, cesium ensemble, Λ -type three-level system

1. INTRODUCTION

With the development of quantum information, quantum communication is becoming the focus of people's study because of its almost absolute safety. Photons are ideal carriers of quantum information transfer and have large potential information capacity, making encoded information robust. In 2001, DLCZ protocol is proposed for the realization of scalable long distance quantum communication¹. Moreover, generation of non-classical photon pairs² and coherent storage and retrieval of sub-nanosecond low-intensity (several thousand photons) light pulses with atomic ensemble advanced quantum networks³. Very recently, Pan *et al* obtained efficient and long-lived quantum memory with cold atoms inside a ring cavity⁴.

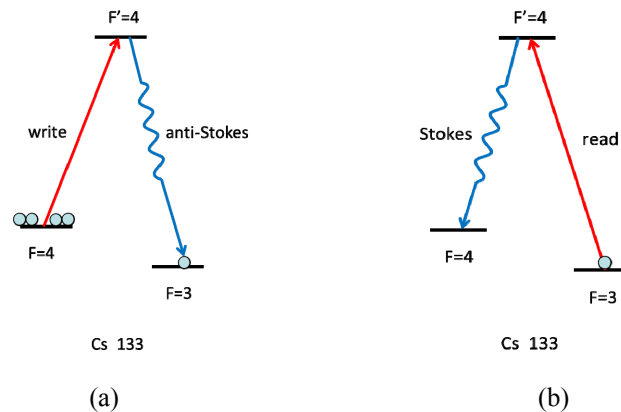


Fig. 1 Relevant Cs hyperfine energy levels for correlated anti-Stokes and Stokes photon pairs based on collective Raman excitation of Cs atomic ensemble.

Most experiments demonstrated so far utilize a Λ -type three-level atomic ensemble by the following sequence in Fig. 1. With atoms initially prepared in $F = 4$ ground state by optical pumping, the “write” laser pulse tuned near the

* Email: wwjjmm@sxu.edu.cn

$6S_{1/2} (F = 4) - 6P_{3/2} (F' = 4)$ hyperfine transition creates a collective Raman excitation with one Cs atom among the ensemble populating on $F = 3$ state and one anti-Stokes photon around frequency $\omega_{3,4}$ emitting at t_1 . After a variable time delay δt , the “read” laser pulse tuned to the $6S_{1/2} (F = 3) - 6P_{3/2} (F' = 4)$ illuminates the atomic ensemble and generates one Stokes photon around frequency $\omega_{4,3}$. These Stokes and anti-Stokes photon pair show a non-classical correlation. Based on this collective Raman excitation of atomic ensemble quantum memory and single photons are demonstrated. In experiment, in order to efficiently detect the single-photon-level Stokes and anti-Stokes photons, the much stronger “write” (“read”) laser pulses which are frequency detuned only ~ 9.2 GHz (Cs case) from the generated anti-Stokes (Stokes) photons must be selectively suppressed or filtered out. Normally people adopt a laser-pumped atomic vapor cell or a confocal Fabry-Perot optical cavity or a bulk etalon to serve as optical filters to meet above-mentioned demands.

Here we report our experimental investigations and characterizations of two kinds of high-contrast optical filters by utilizing a laser-pumped Cs atomic vapor cell and a properly-designed temperature-stabilized Fabry-Perot bulk etalon.

2. ATOMIC OPTICAL FILTER

As shown in Fig. 2, we work with Cs D_2 line at a wavelength of 852 nm. To separate the anti-Stokes photons and excitation channel (“write” pulse), a linearly polarized strong pump laser locked to $6S_{1/2} (F = 3) - 6P_{3/2} (F' = 3)$ drives the atoms populate toward the $6S_{1/2} (F = 4)$ level. The “write” pulse coupled to $6S_{1/2} (F = 4) - 6P_{3/2} (F' = 4)$ hyperfine transition undergoes absorption while the anti-Stokes photons at $6S_{1/2} (F = 3) - 6P_{3/2} (F' = 4)$ hyperfine transition can pass through the medium freely because of optical pumping. In contrast, if pump laser is locked to $6S_{1/2} (F = 4) - 6P_{3/2} (F' = 3)$ hyperfine transition which drives the atoms populate on the $6S_{1/2} (F = 3)$ level, we can pick up Stokes photons from strong “read” pulse. In atomic optical filter, the pump laser intensity is much greater than the saturation intensity of $I_{\text{sat}} = 1.12 \text{ mW/cm}^2$ for Cs D_2 line. The intensity is chosen such that resonant velocity group atoms are efficiently pumped, but other velocity group atoms experience little pumping effect. The pump frequency can be tuned to address a narrow velocity class of atoms, determining the central frequency of our filter within the Doppler width of the transition. The probe laser that is collimated into the cell with the intensity $< 0.1 I_{\text{sat}}$ is used to avoid self-pumping effects on the atoms.

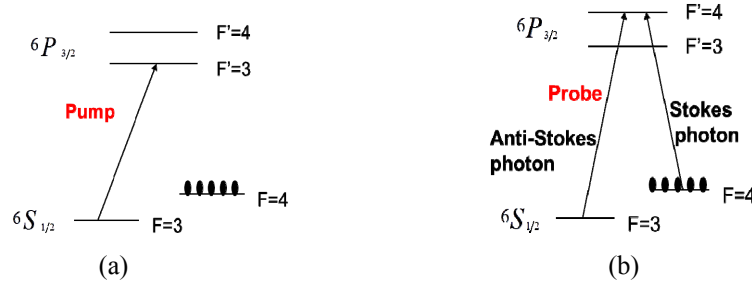


Fig. 2 Relevant Cs hyperfine energy levels for Cs atomic filter. (a) The pump light locked to $6S_{1/2} (F = 3) - 6P_{3/2} (F' = 3)$ hyperfine transition drives the atomic population to the $6S_{1/2} (F = 4)$ level. (b) The Stokes photons (“write” pulse) run on $6S_{1/2} (F = 4) - 6P_{3/2} (F' = 4)$ hyperfine transition and the anti-Stokes photons run on $6S_{1/2} (F = 3) - 6P_{3/2} (F' = 4)$ hyperfine transition.

The experiment setup used in this work is shown in Fig. 3. We used a distributed feed-back (DFB) semiconductor laser as the probe. The probe laser beam is collimated into the cell with the diameter of ~ 2.2 mm. The pump light provided by extended-cavity diode laser (ECDL) is magnified to a diameter of ~ 6 mm before entering the Cs atomic vapor cell. In traditional experiments, probe beams intersect with the pump beam inside the experimental cell at a little crossing angle as shown in Fig. 2(a), a disadvantage of this proposal is the reflected and scattered pump light goes into the detector along with probe light, which is caused by cesium vapor that stick to cell windows⁵. Some experiment groups utilize PBS (change polarization of laser), pin-hole or detector with fiber coupling to reduce the weakness⁶. Here we proposed a new scheme that the pump beam is directed into the cesium cell counter-propagating with the probe beam using a large-surface reflectance-coated mirror with a 3 mm diameter hole drilled at its center in Fig. 2(b)⁷. This design was inspired by the “slow light beam splitter” scheme proposed by Xiao *et al*⁸. Their proposal describes a slow light beam splitter using rapid coherence transport in a paraffin-coated-wall atomic vapor cell. The particles undergoing random and undirected classical motion can mediate coherent interactions between two or more optical modes. In our

realization, we use a hollow pump laser preparing atoms on certain hyperfine ground state, these atoms spread to the middle region via atomic motion and prepared hyperfine states can be preserved. These state-prepared atoms absorb unwanted “write” or “read” laser pulse, while the anti-Stokes (Stokes) photons can pass through the medium freely. At the same time, this design can avoid available the harmful influence induced by the reflected and scattered pump light. Pure Cs atomic vapor is contained in a cylindrical glass cell with a diameter of 25 mm and a length of 75 mm. The windows are anti-reflection coated outside. A magnetic shielding chamber reduces the stray magnetic field to < 40 nT. The vapor cell is heated by the coils using the twisted-pair constantan wires along the cell axis inside the magnetic shielding chamber. The transmission of probe light is 95% when it is far detuned from resonance (cell window loss is $\sim 4\%$).

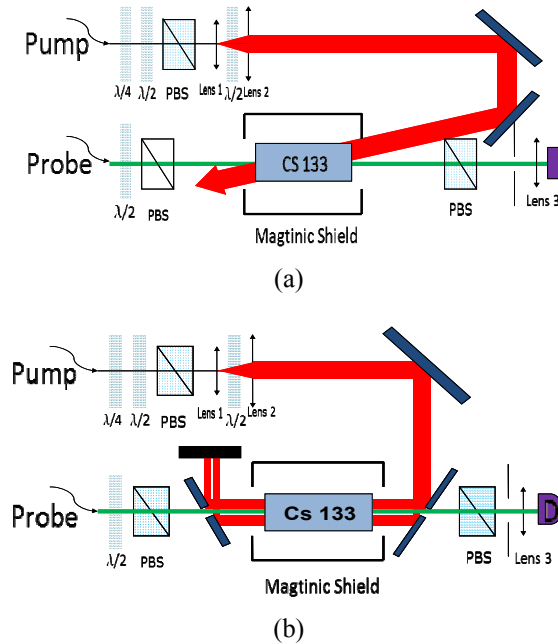


Fig. 3 Schematic diagram of the experimental setup. The pump beam is provided by extended-cavity diode laser (ECDL), while the probe beam is provided by distributed feed-back (DFB) semiconductor laser. Keys to figure: The combination of $\lambda/4$, $\lambda/2$ and PBS is used to provide more P polarization pumping power, and another $\lambda/2$ between lens1 and lens2 changes the polarization to S; the probe laser passes a $\lambda/2$ and PBS to change to P polarization. The polarization of two lasers is vertical. The PBS, pin-hole and lens3 before detector (D) are used to avoid the reflected and scattered pump light. (a) The probe beam intersects with the pump beam inside the experimental cell at a crossing angle less than 2° . (b) The pump beam is directed into the Cs cell counter-propagating with the probe beam by using a large-surface 45° -full-reflection mirror with a 3-mm-diameter hole drilled at the center.

In the experiment, we measured the transmission rate of probe beams as a function of pump beam intensity in Fig 4. A linearly polarized pump laser locked to the $6S_{1/2}$ ($F=3$) - $6P_{3/2}$ ($F'=3$) drives the atom populate at the $6S_{1/2}$ ($F=4$) level. From the view of physical interpretation, the increment of the pump laser intensity can populate more atoms into $6S_{1/2}$ ($F=4$) when the pump laser is unsaturated. According to the selection rules, “write” pulse (Stokes photons) couples the level $6S_{1/2}$ ($F=4$) to the upper state $6P_{3/2}$ ($F'=4$) while the Anti-Stokes photons pass through the atom freely. The peak transmission of anti-Stokes photons increased with the intensity of pumping laser, in contrast, the lowest transmission of “write” pulse (Stokes photons) decreased with the pump intensity. We obtain that the peak transmission of anti-Stokes photons is higher with the hollow pump laser beam than that with solid pump laser beam, it is inversely to the lowest transmission of “write” pulse (Stokes photons). By comparing the distinction ratio between “write” pulse (Stokes photons) and anti-Stokes photons when the core of pump laser is hollow and solid, we can see that the result is better with solid pump laser in Fig. 4(c), above dates are measured at room temperature.

Why the distinction ratio between “write” pulse (Stokes photons) and anti-Stokes photons is lower with hollow pump laser? We realize that the reason is rapid transport of coherent using a wall-coated atomic vapor cell with no buffer gas. Coating glass cell walls with coherence-preserving material such as butter gas and paraffin enable atoms to undergo thousands of wall collisions without destroying their internal state, thus enhancing the coherence lifetime and improve

distinction ratio. At the same time, increasing the pumping intensity and atomic number intensity by heating the vapor are excellent choices.

When increasing the power of pump laser to ~ 44.9 mW, we study the transmission rate of probe light (~ 1 mW) as a function of the cesium medium's temperature in Fig. 5. The transmission rate of probe lasers both decreased at higher temperature of cesium atomic vapor, the peak transmission of anti-Stokes photons can reach $\sim 74.3\%$ and distinction ratio between two probe lasers can reach ~ 26.71 dB at 47.15°C .

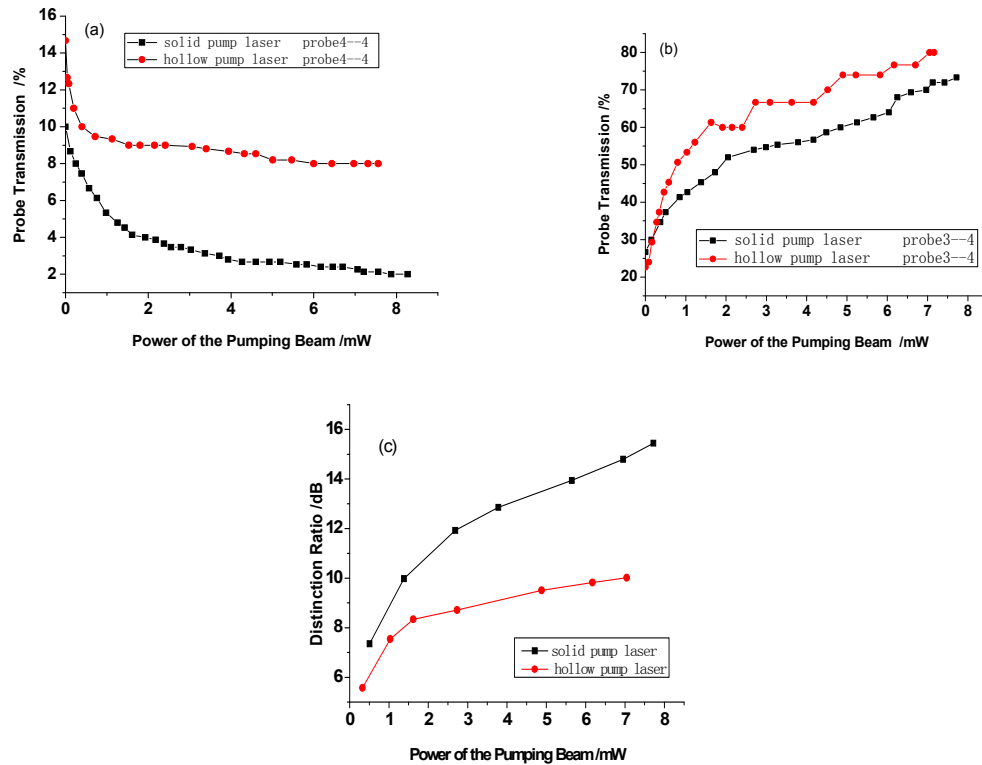


Fig. 4 The peak transmission of the probe as a function of pump intensity at room temperature; black square represents the core of the pump beam is solid. Red diamond represents the core of the pump beam is hollow. (a) (b) The transmission rate of probe beams as a function of pump beam intensity. (c) The distinction ratio between “write” pulse and anti-Stokes photons with hollow and solid pump laser.

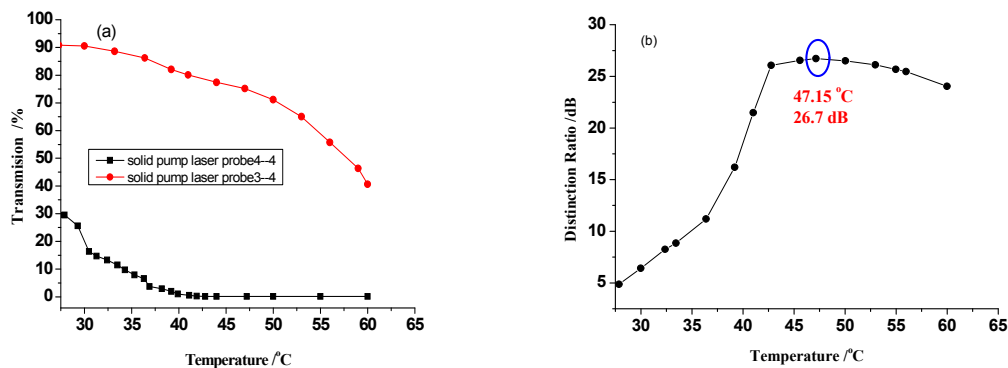


Fig. 5 The transmission of probe lights as a function of Cs vapor cell's temperature when the power of pump laser is 44.9 mW. (a) The transmission of “write” pulse and anti-Stokes photons. (b) The distinction ratio between “write” pulse and anti-Stokes photons.

In atomic optical filter, the center frequency is determined by the pump frequency within the Doppler width of the

transition, so this filter is not competent with two far off-resonant frequency probe lasers. To separate successfully two lasers with the frequency difference of ~ 9.2 GHz and off-resonant, we designed a temperature-stabilized, dozens of GHz resonant transmission tunable laser frequency, narrow band etalon filter⁹.

3. ETALON OPTICAL FILTER

Temperature-stabilized etalon filter is made of K9 glass with a refraction index of 1.509 at 852 nm. We require that diameter is 10mm, maximum error of parallelism is less than $1''$, face type is L/10 and flatness is 20-10. The expansion coefficient α is $\sim 8.7 \times 10^{-6}/K$ when the temperature is between 20 °C to 120 °C. If both surfaces have a reflectance R when the laser wavelength is near 852 nm, the transmittance function of the Etalon without loss is given by:

$$T = \frac{1}{1 + \frac{4R \sin^2(\delta/2)}{(1-R^2)}} \quad (1)$$

Where phase deviation $\delta = 4\pi n l / \lambda$ when the light goes there and back in the etalon, c is light velocity, R is intensity reflectivity, n is the refraction index of the etalon. The laser frequency of peak transmission is $\nu = m \cdot c / (2n l)$. The free spectrum range (FSR) of etalon is $\Delta \nu = c / (2n l)$. The linewidth (full width at half maximum) is following:

$$\Delta \nu_{1/2} = \frac{c}{2n l} \frac{1-R}{\sqrt{R}} \quad (2)$$

To separate successfully two lasers with a frequency difference of ~ 9.19 GHz, we choose the thickness of etalon is 5.433 mm at room temperature, theoretical calculation shows FSR is ~ 18.4 GHz. Fig. 6 shows the transmission rate as a function of laser frequency when laser comes into etalon at 0 degree. We can see that the bandwidth and lowest transmission rate between the two transmission peaks decreased along with the increased reflection rate, but FSR will obtain constant value if the length of lens does not change. When intensity reflection $R = 75\%$, 92% and 99% , we can see that the bandwidth is ~ 1690 MHz, ~ 491 MHz and ~ 60 MHz, respectively. The lowest transmission rate between two transmission peaks is $\sim 2\%$, $\sim 0.18\%$ and $\sim 0.003\%$. To obtain great extinction rate, we prefer to the reflection rate with the lowest transmission between the two transmission peaks. At the same time, the stability of temperature and laser frequency must be considered for the steady-going transmission light. So we decide to select intensity reflection of $R = 92\%$. We assume that thickness of etalon is l_0 at temperature of etalon t_0 , when temperature changes Δt , the length becomes $l = l_0(1 + \alpha \Delta t)$. Theoretical calculation shows FSR can be scanned when the temperature changes 6.33 °C.

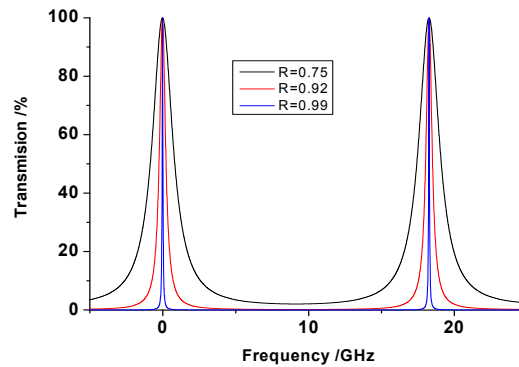


Fig. 6 Calculated transmissivity and corresponding linewidth (full width at half maximum) of the etalon versus laser frequency detuning at different surface intensity reflection of the etalon.

In 2011, our group measured some parameters of etalon which is the same with it used in this paper, but the peak transmission is $\sim 84\%$ ¹⁰, which is far from the theoretically calculated value, so we have improved the structure of holding furnace, as shown in Fig. 7. We employed four pieces Peliter elements to heat or cool etalon for uniform temperature, and Peltier elements are driven by temperature controller with accuracy of 0.5%. Nylon is used for the shell, which isolates furnace from external environment and obtain stable temperature of etalon. The furnace is made of brass

and a thermistor is used to sensor temperature of the etalon. The etalon with a diameter of 10 mm and a thickness of 5.433 mm is made of K9 glass with double-side coatings with reflectivity of 92% at 852 nm.

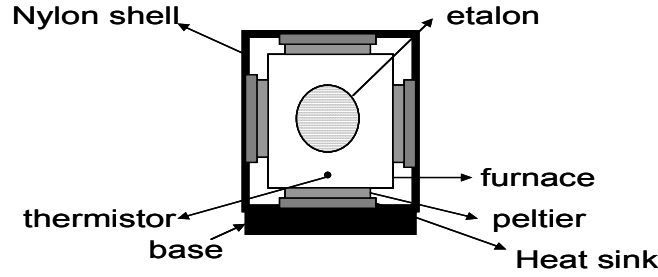


Fig. 7 Schematic diagram of the structure of etalon optical filter. Four pieces Pilter elements to heat or cool the etalon for uniform temperature profile. Nylon is used for the shell. Furnace is made of brass. A thermistor is used to sensor temperature of the etalon.

As known to us, a wanted transmission frequency can be obtained and unwanted frequency can be restrained by changing the temperature of etalon. In experiment we measured transmission rate of probe laser with frequency of $6S_{1/2}$ ($F = 4$) - $6P_{3/2}$ ($F' = 4$) as a function of etalon temperature in Fig. 8. Particularly, the power of output light after etalon and input light power are measured respectively at different temperature of etalon. It is clearly shown that a peak transmission rate of $\sim 91.7\%$ for probe laser can be seen at 25.74°C and lowest transmission rate reaches $\sim 0.16\%$ at 29.13°C , and then the other transmission peak appears when the temperature changes to 32.35°C , so a FSR can be scanned perfectly when the temperature changes 6.61°C , this result can be nearly fit with theory calculation. At the same time, we can see that the transmission rate is higher than it measured before. The reason is probably improved temperature stability and uniformity. So we can conclude from Fig. 8 that a laser that resonant with etalon at proper temperature can be transmitted stability and off-resonant frequency with $2\sim 16$ GHz frequency detuned can be restrained perfectly.

In the detection of non-classical photon pairs by the etalon filter, anti-Stokes with the frequency of $6S_{1/2}$ ($F = 3$) - $6P_{3/2}$ ($F' = 4$) hyperfine transition can be transmitted and “write” pulse with 9.19-GHz frequency-detuned can be restrained at 29.13°C . While in a similar way, Stocks photons can be transmitted and “read” pulse is restrained at the temperature of 25.74°C and 32.35°C excellently.

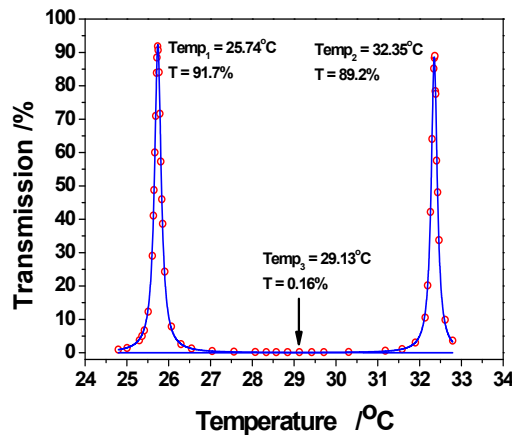


Fig. 8 Transmission of the etalon versus the temperature when the laser frequency is stabilized to $6S_{1/2}$ ($F = 4$) - $6P_{3/2}$ ($F' = 4$) hyperfine transition.

Although distinction ratio between two probe lasers with 9.19GHz-frequency-detuned is a focus we concerned, transmitted power fluctuation of the laser is also a very important parameter in the detection of non-classical photon pairs. We measured transmitted power fluctuation of the laser with resonant frequency in ten minutes in Fig. 9, the fluctuation of transmitted power is $\sim 2.35\%$ which consists of the detector electric noise. We can infer that the stability of laser

frequency and controlled temperature of etalon is excellent. This system is fulfilled with the detection of quantum correlation for photon pairs in a Lambda-type three-level atomic ensemble with Raman excitation

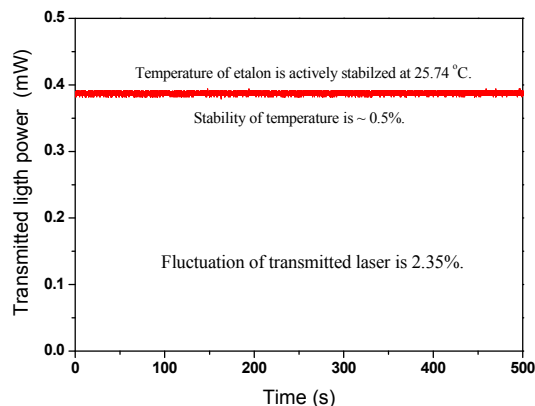


Fig. 9 The optical intensity fluctuation of transmitted laser from etalon.

An outstanding feature of etalon filter is large tunable resonant frequency can be gained accurately by changing the temperature of etalon, so we research the resonant frequency as function of the temperature of etalon in Fig 10. we can see that the peak resonant frequency changes ~ 2.772 GHz when the temperature changes 1°C , which is demarcated by cesium hyperfine spectroscopy, but there are some errors that the slope is not a constant value accurately if we want to get dozens of GHz difference resonant frequency.

From Fig. 8 and Fig. 10, we can figure out that the free spectrum region is ~ 18.32 GHz and the bandwidth is ~ 460 MHz, which is fitted with theoretical calculation perfectly.

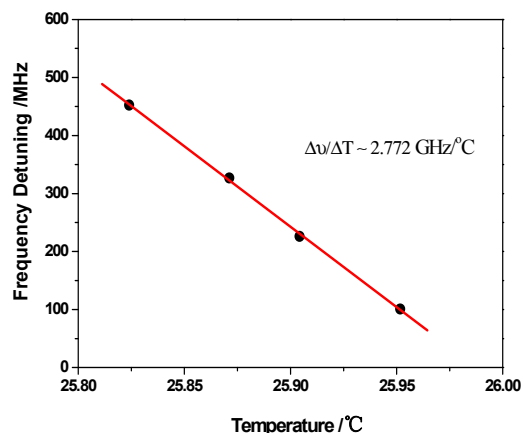


Fig.10 The resonance transmission frequency detuning versus the temperature of etalon.

4. CONCLUSIONS

In conclusion, we have demonstrated two kinds of high-contrast optical filters for the detection of signal lasers which resonant and off-resonant with cesium hyperfine energy level and obtained high distinction ratio, but it is still insufficient for the detection of single-photon-level optical pulses. In order to obtain higher distinction ratio and more narrow bands, some groups tried to use series-wound temperature controlled etalons, but the effect is not beautiful because of the instable output frequency. Some other groups get high distinction ratio by combining atomic optical filter and bulk etalon filter⁴ or multiple-pass temperature-stabilized etalon¹¹ in the experiments. Further more, we assume that it may be a reasonable scheme by using multiple bulk etalons in a temperature controlling furnace.

ACKNOWLEDGEMENT

This work was supported by the National Natural Science Foundation of China (Grant Nos. 60978017, 61078051, 11274213 and 61205215), the National Major Scientific Research Program of China (Grant No. 2012CB921601), the Research Project for Returned Abroad Scholars from Universities of Shanxi Province, China (Grant No. 2012-015) and the Project for Excellent Research Team of the National Natural Science Foundation of China (Grant No. 61121064).

REFERENCES

- [1] Duan L M, Lukin M, Cirac J I and Zoller P, "Long-distance quantum communication with atomic ensembles and linear optics", *Nature* 414, 413 (2001).
- [2] Kuzmich A, Bowen W P, Boozer A D, Boca A C, Chou W, Duan L M and Kimble H J, "Generation of nonclassical photon pairs for scalable quantum communication with atomic ensembles", *Nature* 423, 731 (2003).
- [3] Reim K F, Nunn J, Lorenz V O, Sussman B J, Lee K C, Langford N K and Walmsley I A, "Towards high-speed optical quantum memories", *Nature Photonics* 4, 218 (2010).
- [4] Bao X H, Reingruber A, Dietrich P, Rui J, Duck A, Strassel T, Li L, Liu N L, Zhao B and Pan J W, "Efficient and long-lived quantum memory with cold atoms inside a ring cavity", *Nature Phys.* 8, 517 (2012).
- [5] Liu H L, Hao H Y, Xu Z X, Zhang Z Y, Li S J and Wang H, "The experiment investigation of Rb atom filter", *Acta Sinica Quantum Optica* 18, 291 (2012) (in Chinese).
- [6] Reim K F, Michelberger P, Lee K C, Nunn J, Langford N K and Walmsley I A, "Single-photon-level quantum memory at room temperature", *Phys. Rev. Lett.* 107, 053603 (2011).
- [7] Cere A, Parigi V, Abad M, Wolfgramm F, Predojevic A and Mitchell M W, "Narrowband tunable filter based on velocity-selective optical pumping in an atomic vapor", *Opt. Lett.* 34, 1012 (2009).
- [8] Xiao Y H, Klein M, Hohensee M, Jiang L, Philips D F, Lukin M D and Walsorth R L, "Slow light beam splitter", *Phys. Rev. Lett.* 101, 043601 (2008).
- [9] Cao X M, Yang X D, Li S J and Wang H, "A resonant frequency tunable and narrowband F-P interference filter controlled by the temperature", *Acta Sinica Quantum Optica* 14, 72 (2008) (in Chinese).
- [10] Li Z H, Li G, Zhang Y C, Zhang P F, Zhao D M, Guo Y Q, Wang J M and Zhang T C, "Generation of Raman laser for STIRAP of cesium atom", *Acta Optica Sinica* 31, 0102002 (2011) (in Chinese).
- [11] Hockel D and Benson O, "Electromagnetically induced transparency in cesium vapor with probe pulses on the single-photon level", *Phys. Rev. Lett.* 105, 153605 (2010).